RESONANCE HAMMER DRILLING: STUDY OF A VIBRO-IMPACT SYSTEM WITH EMBARKED FORCE

Romulo R. Aguiar, romulo@mec.puc-rio.br
Hans I. Weber, hans@mec.puc-rio.br
Mechanical Engineering Department, PUC-Rio
Rua Maquês de São Vicente, 225, Gávea
22453-900, Rio de Janeiro - RJ - Brazil

Abstract. *Hard rock drilling is still a great challenge for oil companies. Optimum productivity is possible by combining advantages of both rotary and percussive drilling. In this way, besides the rotative penetration, where the teeth of the bit penetrate in the rock when the drillstring rotates, the percussion action creates indentation in the formation, thus this method requires less thrust and power. PUC-Rio University and CSIRO Petroleum are proposing the development of a new drilling technique called* **Resonance Hammer Drilling***. The performed activities correspond to the design and the development of a shaker device called by us "RIMD"(**R**esonant **IM**pact **D**evice) for rotary drilling with a roller-cone bit. The purpose of this work is the experimental study of this drilling technique, where the experiment is focused on the study of impact forces when these are embarked on the main system. Differently from the previous performed experiments, where the RIMD was impacting against a rigid support mounted separately from the main system, now the impact forces will act fully on the main system, which is more representative of the real size system, where the RIMD will be mounted inside the bottom hole assembly of an oilwell drillstring. Finally, the experiment will be used to validate an analytical model that will allow further investigations on this subject providing the way to other RIMD possible constructions.*

Keywords: *nonlinear dynamics, vibro-impact, oilwell drillstrings*

1. INTRODUCTION

It is well known that vibration in drilling leads to failure of drill pipes, intensive bit wear and to an increase of overall cost. Drillstring vibration is complex in nature and couples axial, bending and torsional vibration. Investigations of vibration in drilling are carried out generally by studying each aspect independent of others. To eliminate the negative effects of the vibration, improvements are constantly brought in, through new concepts of drilling and new designs. These new approaches have to consider the efficient use of energy as an important factor, bringing an increase in bit life, in rate of penetration and reduced cost in hard rock drilling.

Conventional rotary drilling is the most economical in comparison with other methods and typically drills holes of up to 850 mm in diameter. It can drill up to 10,000 m deep in almost all formations. In rotary drilling, cutting of rock is achieved by a rotating drill bit under load. Material is removed in the form of dust or chips as a result of the scraping and shearing action of the cutting edges. To obtain big chips and a high rate of penetration, more thrust is required. Hence, this method of drilling suffers from twisting and breakage of the pipes.

Percussive drilling fragments rock formations by means of blows, which occur only for a fraction of time. This method relies entirely on crack propagation and brittleness of the formation because in this case bit rotation does not contribute to the cutting process. If load is inadequate, the rate of penetration decreases due to small chip formation and energy is wasted. However, percussion drilling is preferable in very hard sedimentary rocks, due to low bit wear and fast penetration, but this method cannot produce the same rate of penetration when drilling at greater depth. Moreover, percussive drilling can produce only small holes in diameter.

In this context, optimum productivity is possible by combining advantages of both rotary and percussive drilling. Percussive-rotary drill is not new and was developed first by the Salzgitter Company and then by Hausherr and Nusse & Grafer in 1956. This type of machine has been mainly used in underground works and has shown to have advantages of both drilling methods. More recently, the concept of vibro-impact drilling introduced in the last decades, has proven to be highly promising. Therefore, besides the rotative penetration, where the teeth of the bit penetrate in the rock when the drillstring rotates, the percussion action creates indentation in the formation, thus this method requires less thrust and power. Thus, PUC-Rio University and CSIRO Petroleum are proposing the development of a new drilling technique called ***Resonance Hammer Drilling***.

This technique has as premise to use the already existent vibrations in the drillstring, in fact the axial vibration due to the cutting process, to generate a harmonic load on the bit and an excitation in a steel mass (hammer). When this excitation frequency is near to the steel mass resonance frequency and, since the steel mass displacement is limited in positive direction by the gap, impacts on the bit occur. Therefore, besides the rotative penetration, where the bit teeth penetrate the rock when the drillstring rotates, a percussive penetration happens due to the impact of the hammer with the bit, increasing the ROP. However, the impulsive force generated by the hammer should never be larger than the preload (WOB), due to the possibility of the bit bounce effect. Moreover, the hammer resonance frequency should not coincide

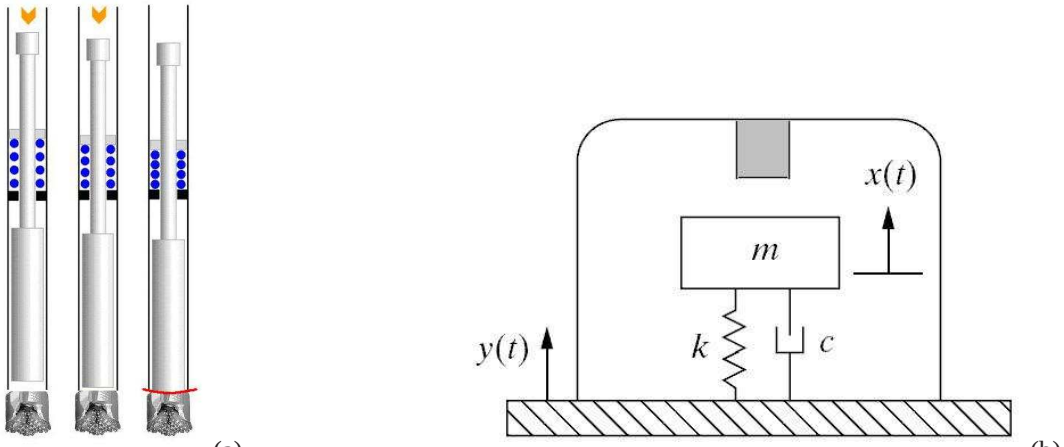

(a) (b)

Figure 1. a) Resonance hammer drilling technique.; b) Vibro-impact system.

with any drillstring natural frequency.

A first investigation of RHD is presented by Franca and Weber (2004). In this work, a model for the longitudinal behavior of the bit-rock with a vibro-impact system is investigated. As conclusion, the behavior of period-1 with one impact per cycle was always the best condition of penetration, increasing the ROP.

A second investigation is presented by Aguiar and Weber (2006, 2007). In this work, a new mechanism to enhance the drillstring rate of penetration is investigated. It is presented a test rig simulating the RIMD performance and the drillstring behavior influence on the RIMD. A numerical modeling with experimental validation is also studied in order to predict the impact forces.

2. OBJECTIVES

The idea in the investigations that were previously performed is that it is possible to obtain this load with the help of the rotary motion and the axial dynamics of the drillstring. To work out a first prototype that synthesizes all this ideas, the development must address the following points: it is needed an impact mass, that shall have very low damping on its motion in order to generate considerable amplitudes, which will be reduced through a gap and cause the impacts. The essential idea of the RIMD is observed in Fig 1(b).

Previous prototypes were studied at the Dynamics and Vibration Laboratory at PUC-Rio, where in all RIMD arrangements the hammer was always impacting against a rigid support. These previous experiments were important to characterize the impact force generated by the hammer under different stiffness/gap combinations and under different excitation frequencies. However the RIMD concept shall be reduced to a device to be mounted on a vibrating structure, which means that impacts will be embarked. In other words, it is necessary to take into account the the impact surface is vibrating with the entire structure.

The construction of this prototype includes obtaining its characteristics, like the range of possible frequencies and the measurement of the generated impulsive forces. This work presents the first experimental data regarding the vibro-impact system where the impact force is embarked. Also, a simple one-degree-of-freedom analytical model is proposed in order to predict the RIMD phenomena.

3. MATHEMATICAL MODELING

For the RIMD analysis, it will be necessary to incorporate the influence of the bit-rock interaction over the drillstring axial vibration behavior. For the bit-rock interaction, it is know that roller-cone bits, during the cutting process, generate an axial smooth movement of the drillstring with a frequency that is n times the rotary speed, where n represents the number of rollers (Dykstra, 1996). In most cases, $n = 3$. In this first approach, the bit-rock interaction will be modeled as a base excitation acting directly on the RIMD.

The first RIMD prototype may be modeled as a single degree-of-freedom with a base excitation where the impact surface is also moving with the system, once the impacts are embarked. The RIMD stiffness is provided by steel beam springs and the damping factor is associated to small friction losses and material damping.

For the impact force, the contact model used here is proposed by Hunt and Crossley (1968), which consists of a nonlinear spring in parallel with a nonlinear damping. The contact force, F_i, is established by the following equation:

$$F_i(\delta, \dot{\delta}) = -k_i\delta^n - c_i\delta^n\dot{\delta} = -k_i\delta^n(1 + \lambda_i\dot{\delta}) \;\; with \;\; \lambda_i = \frac{c_i}{k_i} \tag{1}$$

Where δ is the penetration, $\dot{\delta}$ the penetration velocity, k_i the contact stiffness and c_i some viscous damping. The factor n depends on the geometry characteristics of the contact surface. An important aspect of this model is that damping depends on the penetration. This is physically sound since contact area increases with deformation and a plastic region is more likely to develop for larger penetrations. Another advantage is that the contact force has no discontinuities at initial contact and separation, but it begins and finishes with the correct value of zero. This model has been studied and used by several authors and experimentally the model with a non-linear damping term represents quite well the real behavior of the system during impact (Gilardi and Shaft, 2002).

For the prototype where the impact force is embarked, the first approach for the mathematical modeling is described below.

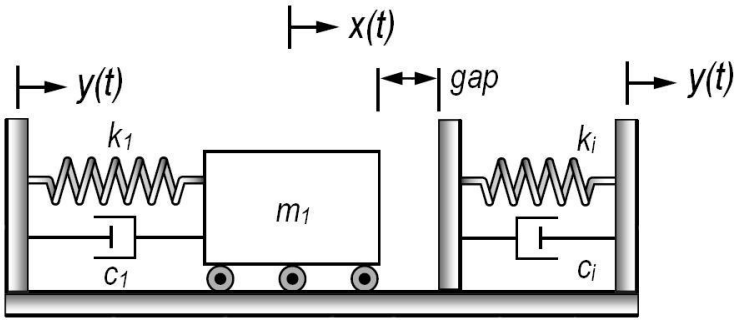

Figure 2. RIMD modeling.

The mathematical modeling considers the hammer (RIMD) as a single degree-of-freedom system, moving on the axial direction ($x(t)$). The cart movement is prescribed in the form:

$$y(t) = Y_0 \sin(\Omega t) \tag{2}$$

Once the impact device is embarked on the moving system, the impact surface movement is also described by $y(t)$. In this way, when the hammer is not impacting the contact surface, its dynamics is described by:

$$m\ddot{x} + c\dot{x} + kx = cY_0\Omega\cos(\Omega t) + kY_0\sin(\Omega t) \tag{3}$$

Where the contact condition is givenby:

$$x \geq Y_0 \sin(\Omega t) + gap \tag{4}$$

The impact forces are given by the Hunt and Crossley model, Eq. 1, where the penetration δ is described by:

$$\begin{aligned} \delta &= x - y - gap \\ \dot{\delta} &= \dot{x} - \dot{y} \end{aligned} \tag{5}$$

Therefore, the dynamics equation for the impact condition is shown below:

$$m\ddot{x} + c\dot{x} + kx = cY_0\Omega\cos(\Omega t) + kY_0\sin(\Omega t) - k_i\delta^n - c_i\delta^n\dot{\delta} \tag{6}$$

which becomes a nonlinear dynamic problem due to the discontinuity and impact. All simulations were solved using a 5th order Runge-Kutta method. Once the tolerances used during the simulations were extremely tight (10^{-9}), no interpolation was used to determine the point of contact, since this tolerance is narrow enough to produce satisfactory results.

4. EXPERIMENTAL RESULTS

4.1 Test rig apparatus, methodology and parameter identification

The experimental apparatus attempts to represent the drillstring axial behavior and its influence over the impact device (RIMD), according to the simplifications previously discussed. The experimental apparatus is show on Fig. (3).

The experiment consists in a main cart, which can slide in the horizontal axis over a low friction rail assembly, excited by an AC motor. The motor is attached to the cart through a pin that can slide over a groove machined on a plastic plate fixed on the cart. Once the pin hole is drilled off-centered on the rotating disk, the rotational movement of the motor is

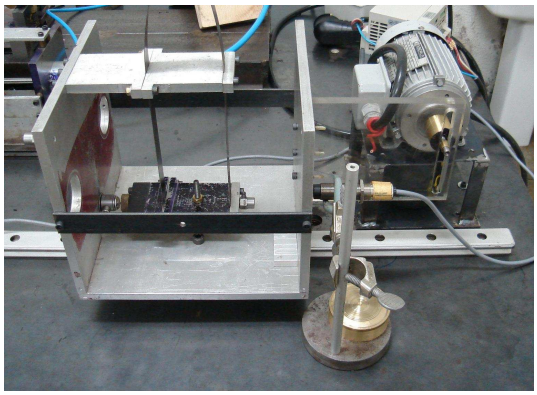

(a)

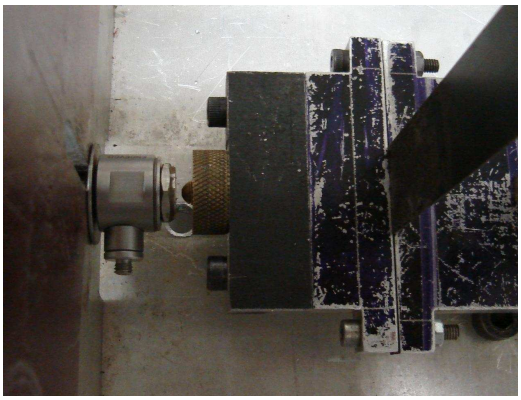

(b)

Figure 3. Experiment Photos: a) Entire test rig; b) Impact device.

turned into a perfectly sinusoidal cart movement. The reason why such device was used instead of a shaker is that with the actual device there can be developed higher amplitudes (not achievable with a shaker) but mainly because it is intended to avoid the influence of the impact forces on the excitation in higher frequencies, experience gained in previous experiments set ups.

Inside the cart is fixed the RIMD, i.e., a mass-spring system attached to the cart, moving on the horizontal direction. The RIMD stiffness is assured by two clamped-clamped bending beams (steel) coupled to the cart by aluminum couplings. These beams has a transverse section of 22.3 mm width and 0.6 mm height. The length of these beams can be changed in order to vary the RIMD stiffness. The RIMD mass is composed by one of the aluminum couplings and by the impact device (steel). In order to change the gap between the RIMD and the cart, the impact device is composed by a long screw and a knurled nut, as shown on Fig. (3b).

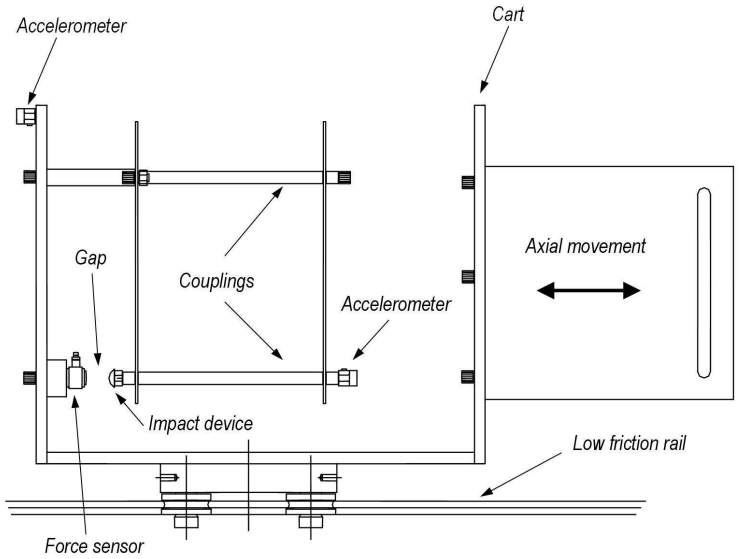

Figure 4. Experiment Sketch.

The test rig is instrumented with two accelerometers, one fixed to the cart (accelerometer Endevco 751-10 SN AC28) and the other one attached to the RIMD (accelerometer Endevco 751-10 SN AC69); one piezoelectric force sensor (Endevco 2311-100 SN 2471), fixed on the cart and located in front of the RIMD impact device; and one displacement sensor (Balluff standard inductive sensor), in a way to measure the cart movement (to check if the impact forces have any influence on the excitation). Therefore the output parameters are the cart displacement and acceleration, RIMD acceleration and the impact force.

The difference from previous experiments is that we tried to keep the excitation force free from the effects of the impacts.

The experiment parameters are:

- RIMD stiffness, as the beam length is varied;

Table 1. Sensor specs.

Cart Accelerometer - 751-10 SN AC69		
Sensitivity	10.194	mV/g
Measure Range	± 50	g
Resonance frequency	50	kHz
RIMD Accelerometer - 751-100 SN AC28		
Sensitivity	111.68	mV/g
Measure Range	± 50	g
Resonance frequency	50	kHz
Impact Force Sensor - 2311-100 SN 2471		
Sensitivity	24.41	mV/N
Measure Range	± 220	N
Resonance frequency	75	kHz

- the impact device gap, with the knurled nut and screw, measured through a calibrated shim.

The input parameter is the excitation frequency from the AC motor, where the pin is drilled 1mm off-centered. The outputs are:

- acceleration signals from accelerometers mounted in different points of the test rig, according to Fig. (4).
- the impact force applied by the RIMD.
- the cart displacement, measured through an inductive displacement sensor.

The methodology applied is to observe the behavior of the impact system as the RIMD stiffness is decreased and the gap is varied. The results shown in this work are for the same RIMD stiffness, changing only the gap. For this value of stiffness, the natural frequency of the system without impact is determined, as well as the system parameters.

After that, a study with impact is carried out. The excitation frequency from the AC motor is changed in order to sweep the range of the system natural frequencies.

For the masses, stiffness and damping, the parameter identification of the test rig follows the literature existing modal analysis and logarithmic decrement. For the impact coefficients (Hunt and Crossley impact model), a smaller experiment was performed, where a well known initial condition was imposed to the system and the experimental response was compared to the response of the equivalent mathematical model, where the impact model coefficients were adjusted.

4.2 Experimental results

First, for the system without impact, the parameters are identified and the natural frequency is obtained. These results are shown on Tab. (2). The study of the system without impact is considered in order to determine which range of frequencies will be swept, so all characteristics of the system with impact are observed.

Table 2. Parameters identification - couplings distance 160 mm.

Natural frequency	ω	4.63	Hz
Total Mass (cart + RIMD)	m	5.38	kg
Stiffness	k	272.5	N/m
Damping	c_1	0.060	Ns/m

System with impact, gap 0mm

Following the same methodology applied in previous experiments, it will be observed the behavior of the impact system as the RIMD stiffness is increased and the gap is varied. As mentioned, for the masses, stiffness and damping, the parameter identification of the test rig follows the literature existing modal analysis and logarithmic decrement. For the impact coefficients (Hunt and Crossley impact model), the parameters used are the same as identified in a previous experiment (Aguiar and Weber, 2007), once the impact force sensor and the RIMD device are exactly the same.

As observed in all stiffness/gap combinations, similar to what was observed in the previous experiments (Aguiar and Weber, 2007), the RIMD behavior can be divided in several frequency bands, in this particular case two separate bands, showing similar characteristics in each frequency band in all combinations. In the first excitation frequency (4 to 5Hz), the impact force presents a period-2 behavior, with small impact forces, as it is shown on Fig.(5).

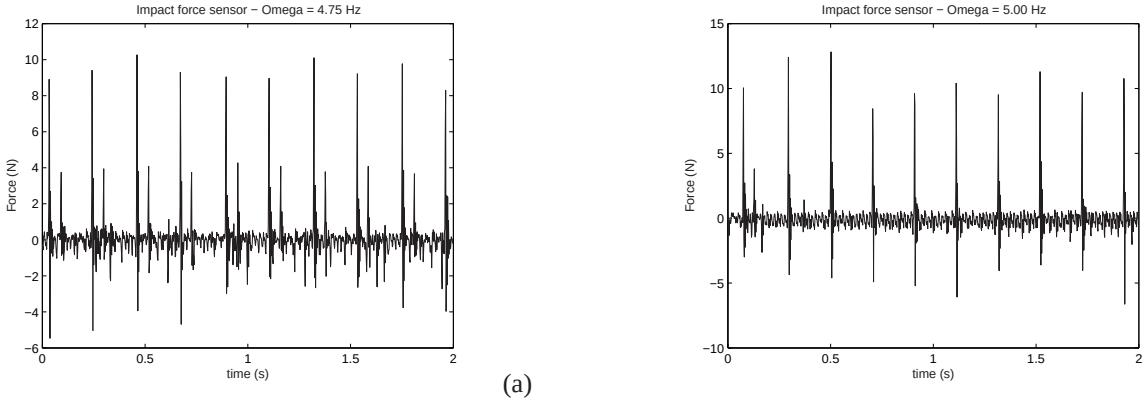

(a) (b)

Figure 5. Impact behavior transition; Impact force over time; Couplings distance 160 mm; gap 0mm; a) $\Omega = 4.75Hz$; b) $\Omega = 5.00Hz$.

From 5 Hz until 11 Hz, the maximum excitation imposed to the system, the impacts present a period-1 behavior, increasing the value of the maximum impact force until the frequency of 9.5 Hz, where the system experiences the maximum impact force (61 N). After passing through the resonance, the impact force decreases its value. On Fig. (6) it is shown the evolution of the impact force over the excitation frequency.

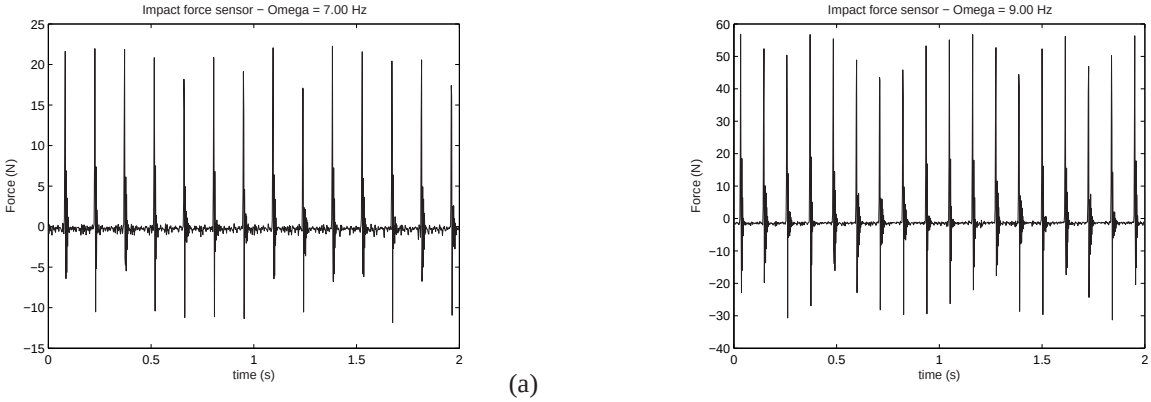

(a) (b)

Figure 6. Time response. Impact force; Couplings distance 160 mm; gap 0mm; a) $\Omega = 7.00Hz$; b) $\Omega = 9.00Hz$.

Differently from previous experiments, one important fact regarding this experiment is that excitation is not influenced by the impacts, an important point that other experiments could not reproduce, specially during the resonance frequencies. This is proven by showing the cart displacement sensor signal under different excitation frequencies, including the frequency where the impact force is maximum. These charts are shown on Fig. (7).

With these data it is possible to analyze the system behavior in the frequency domain. For that, a computational routine is created so as to determine the F_i e F_0 values for each frequency studied. For the F_0 value, once the excitation force is cyclic, the amplitude value is adopted, Eq. 7. For F_i, the maximum value is extracted. This routine to determine the impact force can mask the real results, since on certain frequency bands the impact force peaks do not reveal as constant and there are transitions in the behavior of the impact force. However, the purpose of this analysis is to obtain the optimal parameters that maximize the impact force and, according to what was seen in the experimental data analysis, the impact force reveals itself as periodic and constant on the frequency bands around resonance. Thus, despite the fact that the technique of obtaining only the maximum impact force values masks certain impact conditions (chaotic behavior, for instance), the analysis is valid as long as the main purpose is to determine the system optimal parameters which maximize the impact force and that, under these conditions, the F_i maximum force is constant.

Finally, for making the non-dimensional chart so as to compare it to the answers in the other configurations, the force ratio F_i/F_0 is used. Now, once the displacement is imposed, the maximum impact force will be divided by:

$$F_0 = m_{tot}\, A_0\, \Omega^2 \tag{7}$$

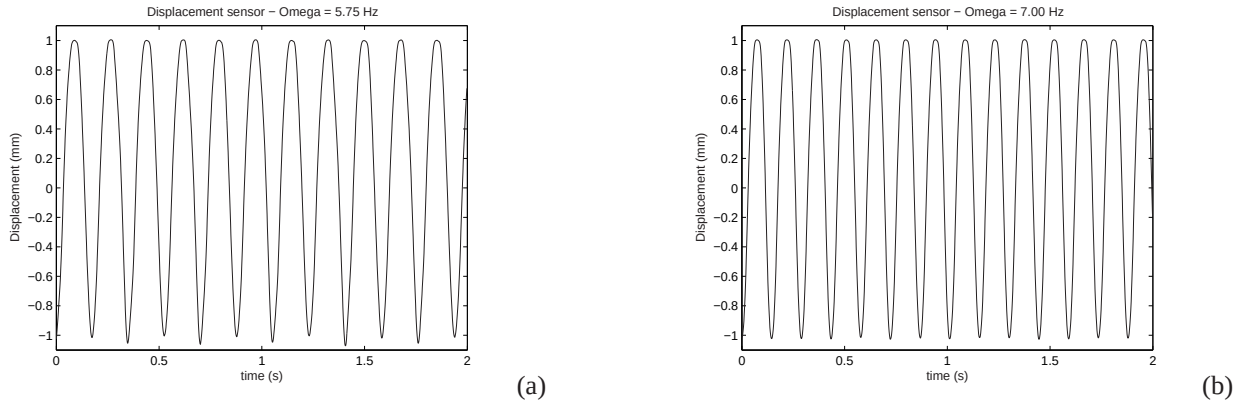

(a) (b)

Figure 7. Time response. Cart displacement; Couplings distance 160 mm; gap 0mm; a) $\Omega = 5.75Hz$; b) $\Omega = 7.00Hz$.

where m_{tot} is the total mass (cart and RIMD inertias), A_0 is the displacement amplitude and Ω is the excitation frequency. This comes from the double differentiation of the imposed displacement ($Y = A_0 sin(\Omega t)$). This is the maximum value of the excitation force.

Therefore, for this stiffness/gap combination, the impact force chart and the force ratio chart (F_i/F_0) in the frequency domain is shown in Fig. (8).

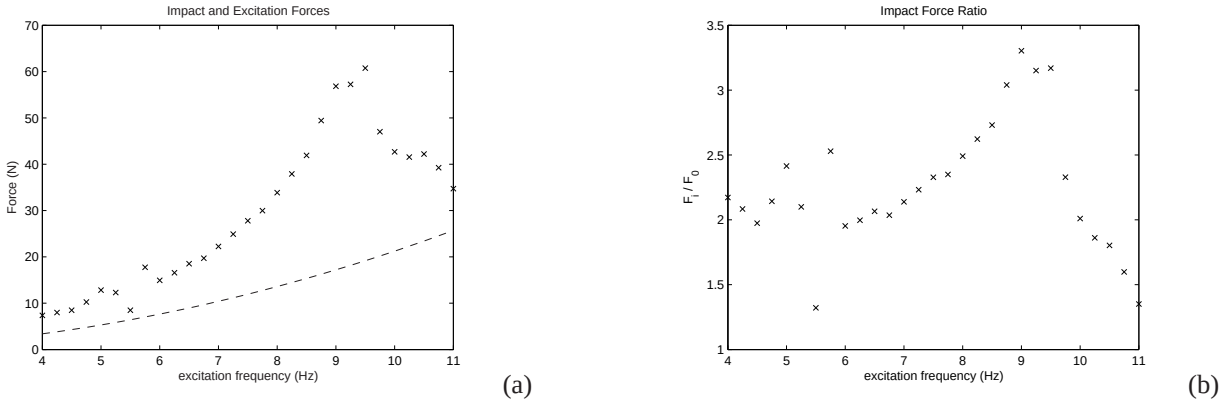

(a) (b)

Figure 8. Frequency domain response. Couplings distance 160 mm; gap 0mm; a) Maximum impact force (x) and excitation force (-); b) Nondimensional force F_i/F_0.

Regarding the charts on Fig. (8), it is noticed that the impact force is low for the first excitation frequencies, increasing its value as the frequency increases, reaching a peak of maximum impact force at 9.5 Hz, which it is called the system resonance, defining resonance as the frequency where the system reaches the maximum impact force ratio, once the displacement is limited by a gap. After the resonance, the maximum impact force decreases as the excitation frequency increases.

Another interesting phenomenon to be noted here concerns the system natural frequencies without and with impact. The presence of the impacts significantly altered the system resonance, as it can be observed on the table (3). This alteration of resonance due to the impacts presence was already studied (Mattos and Weber, 1997) and was expected.

System with impact, gap 1mm

Similar to the previous gap results, in this configuration it is noted the two frequency bands observed previously, one in initial frequencies showing a period-2 impact behavior (Fig.(9)a) and a second one showing a period-1 impact, where the maximum impact force occurs (Fig.(9)b). However, the presence of a non-zero gap made appear a third frequency band in higher frequencies (after the first resonance), where impacts have a chaotic behavior (Fig.(10)). Once again, the excitation is not influenced by the impacts (Fig.(11)).

Finally, it is show on Fig. (12) the impact force behavior in the frequency domain.

System with impact, comparison among gaps

The same experimental methodology was applied for the 3mm gaps, keeping the RIMD stiffness constant. Therefore, it is possible to compare the impact force for each chosen gap, keeping constant the RIMD stiffness, in the frequency

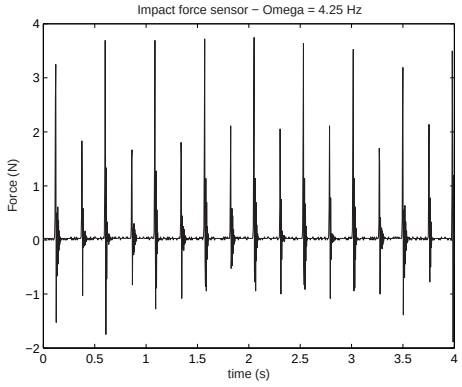

(a)

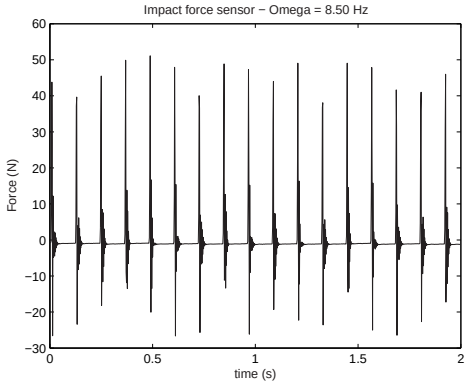

(b)

Figure 9. Impact behavior transition; Impact force over time; Couplings distance 160 mm; gap 1mm; a) $\Omega = 4.25Hz$; b) $\Omega = 8.50Hz$.

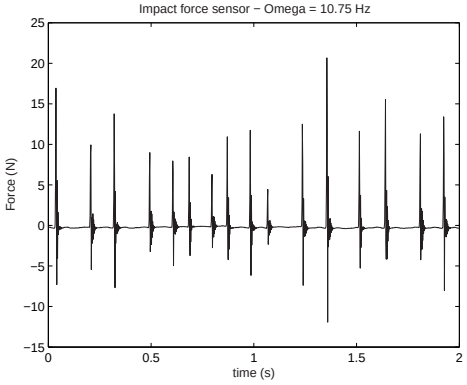

(a)

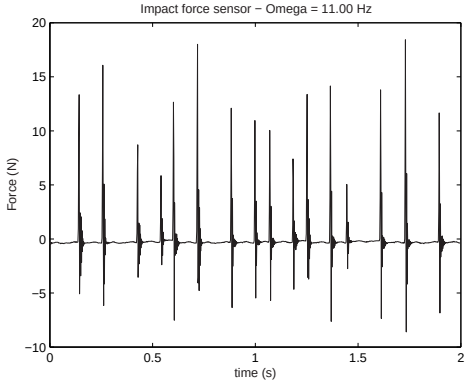

(b)

Figure 10. Time response. Impact force; Couplings distance 160 mm; gap 1mm; a) $\Omega = 10.75Hz$; b) $\Omega = 11.00Hz$.

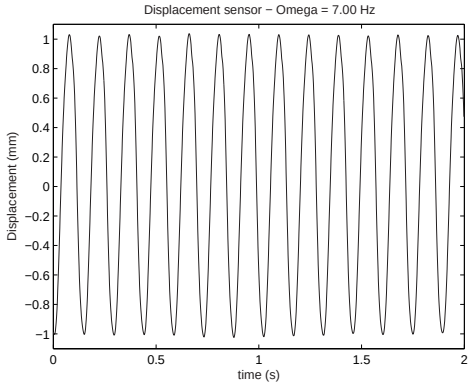

(a)

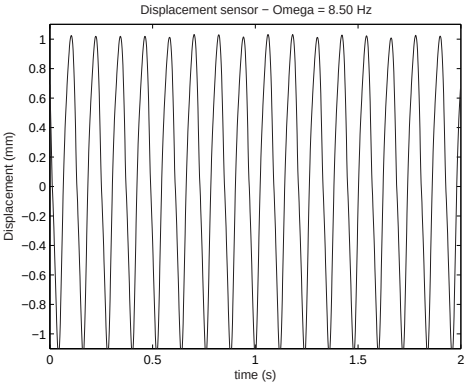

(b)

Figure 11. Time response. Cart displacement; Couplings distance 160 mm; gap 1mm; a) $\Omega = 7.00Hz$; b) $\Omega = 8.50Hz$.

domain. The charts are shown in Fig. (13).

At this point two interesting facts can be addressed. Once again, as seen previously, it can be noticed a variation of resonance frequency as the gap varies (Tab. (3)). However, the most interesting factor is regarding the maximum impact force. In absolute terms, the maximum impact force, for this particular stiffness, is reached when the gap is 00 mm. However, when the impact force becomes nondimensional, it is found that maximum impact force is for the 03 mm gap. This happens because the maximum impact force for the 00 mm gap is reached at a higher frequency than the maximum impact force for the 03 mm gap, therefore the excitation force is also higher, according to Eq. (7). On Tab. (3) is shown the resonance frequencies for the free vibration system and for each gap.

5. MATHEMATICAL MODEL VALIDATION

This section aims at validating the numerical model shown in the previous section through numerical-experimental comparison. The test rig attempts to represent the drillstring axial behavior and its influence on the impact device (RIMD),

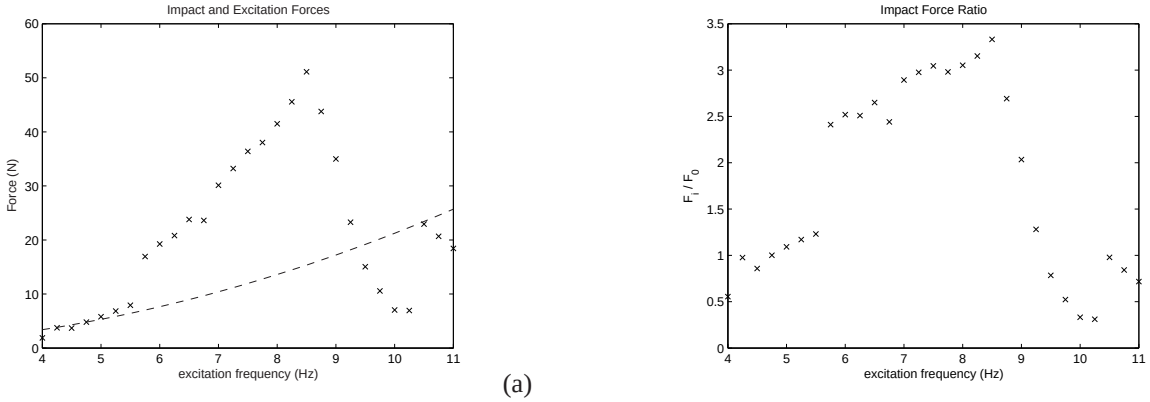

(a) (b)

Figure 12. Frequency domain response. Couplings distance 160 mm; gap 1mm; a) Maximum impact force (x) and excitation force (-); b) Nondimensional force F_i/F_0.

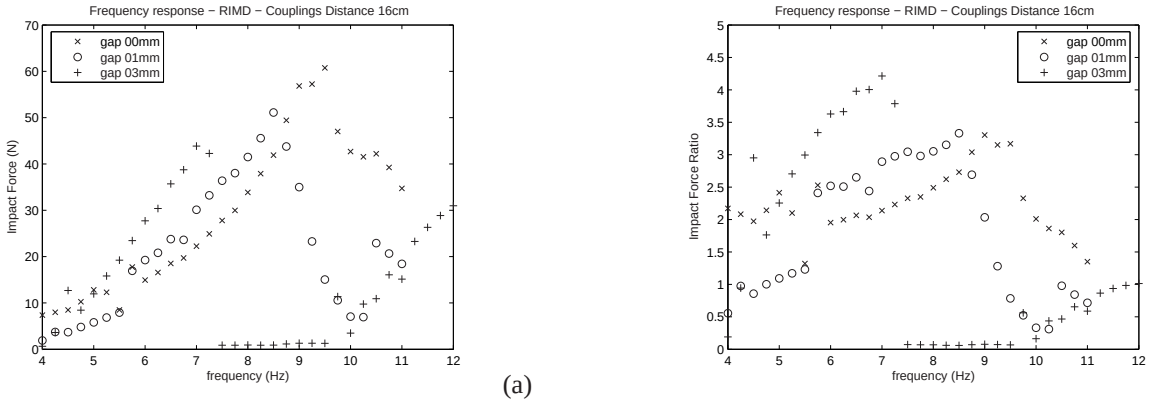

(a) (b)

Figure 13. Frequency domain response. Couplings distance 160 mm; comparison among gaps; a) Impact force; b) F_i/F_0.

Table 3. Resonance frequencies (experimental) - system with and without impact, couplings distance 160 mm.

Natural frequency	
Gap 0mm	9.5 Hz
Gap 1mm	8.5 Hz
Gap 3mm	7.0 Hz
No impact (gap $\rightarrow \infty$)	4.6 Hz

according to the simplifications proposed before. The results are shown below.

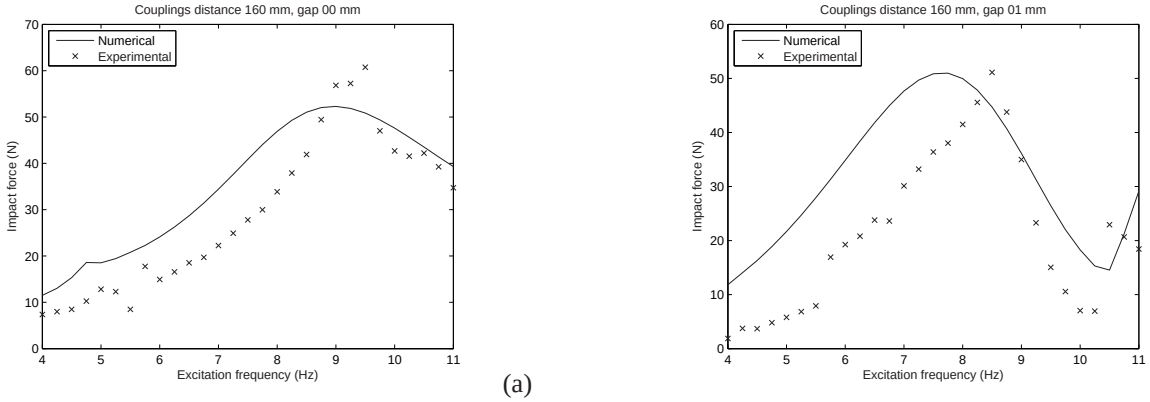

(a) (b)

Figure 14. Frequency domain response. Numerical-experiment comparison; couplings distance 160 mm; a) gap 00mm; b) gap 01mm.

What can be observed from the chart on Fig. (14) is that the numerical results are close to the experimental data, but

without satisfactory results. Another fact is that the numerical results become more inaccurate as the gap increases. In this way there exists two alternatives to improve the numerical model: one is to change the impact force model, and the second alternative is to use the finite element model, once the actual model describes a continuous system (two flexile beams, Fig. (3)) as only a one degree-of-freedom system. This approximation is probably the main reason why the numerical results are not satisfactory.

6. CONCLUSIONS

This article presented the proposal and design of a new device to enhance the rate of penetration in hard rock drilling, called **resonance hammer drilling**. A test rig was designed and built in order to incorporate the RIMD and reproduce the bit-rock interaction in the drillstring axial vibration behavior.

The basic idea in this application is to use the natural vibration of a primary system to induce vibrations in an embarked device, which has a low damping and is able to vibrate and impact on the primary system. The shock wave due to this hammer effect can be used to loose the system from a stick condition. It can also be of value if some brittle material is being cut.

On the experimental analysis, while studying the impact force characteristic, sweeping the excitation frequency, it was noted that, in all stiffness/ gap combinations, there was a certain standard of system behavior which could be divided in frequency bands.

Although the model is not capable to describe all phenomena observed in the experimental analysis, the numerical answer somehow follows the experimental data. There are still some open issues to improve the numerical model in order to reproduce the experimental results.

7. ACKNOWLEDGEMENTS

The authors wish to thank CNPq, FAPERJ and CSIRO for their support of this research.

8. REFERENCES

Aguiar, R.R. and Weber, H.I., 2007, "Development of a vibro-impact device for the resonance hammer drilling", Proceedings of the XII DINAME. Ilhabela, SP, Brazil.

Aguiar, R.R., 2006, "Desenvolvimento de um Dispositivo Gerador de Vibro-impacto", MSc Thesis, Department of Mechanical Engineering, PUC-Rio, Rio de Janeiro, Brazil.

Aguiar, R.R. and Weber, H.I., 2005, "Optimum Parameters of a Vibro-impact Device", Proceedings of the XXVI CILAMCE, Guarapari, ES, Brazil.

Detournay, E., 2004, "Enhanced Bit Performance through Controlled Drillstring Vibrations - Phase 3", Technical Report, Drilling Mechanics Group, CSIRO Petroleum, Bentley, WA, Australia.

Dykstra, M.W., 1996, "Nonlinear Drillstring Dynamics", PhD Thesis, Department of Petroleum Engineering, University of Tulsa, Oklahoma, USA.

Franca, L.F.P., 2004, "Perfuração Percussiva-Rotativa Auto–Excitada em Rochas Duras", PhD Thesis, Department of Mechanical Engineering, PUC-Rio, Rio de Janeiro, Brazil.

Gilardi, G. and Sharf, I., 2002, "Literature survey of contact dynamics modeling", Mechanism and Machine Theory.

Hunt, K.H. and Crossley, F.R.E., June 1968, "Coefficient of Restitution Interpreted as Damping in Vibroimpact", Journal of Applied Mechanics - Transactions of the ASME, pgs 440 to 445.

Mattos, M.C. and Weber H.I., 1997, "Some Interesting Characteristics of a Simple Autonomous Impact System with Symmetric Clearance", ASME - Design Engineering Conference.

Savi, M.A., Franca, L.F.P. and Weber, H.I., 2005, "Nonlinear Dynamics and Chaos of a System with Discontinuous Support Using a Switch Model", Proceedings of the XI DINAME, Ouro Preto, MG, Brazil.

9. Responsibility notice

The author(s) is (are) the only responsible for the printed material included in this paper